

Generative Editing in the Joint Vision-Language Space for Zero-Shot Composed Image Retrieval

Xin Wang^{1,2*} Haipeng Zhang^{2*} Mang Li² Zhaohui Xia²
 Yueguo Chen¹ Yu Zhang^{2†} Chunyu Wei^{1†}

¹Renmin University of China ²Alibaba Group

Abstract

*Composed Image Retrieval (CIR) enables fine-grained visual search by combining a reference image with a textual modification. While supervised CIR methods achieve high accuracy, their reliance on costly triplet annotations motivates zero-shot solutions. The core challenge in zero-shot CIR (ZS-CIR) stems from a fundamental dilemma: existing text-centric or diffusion-based approaches struggle to effectively bridge the vision–language modality gap. To address this, we propose **Fusion-Diff**, a novel generative editing framework with high effectiveness and data efficiency designed for multimodal alignment. First, it introduces a **multimodal fusion feature editing** strategy within a joint vision-language (VL) space, substantially narrowing the modality gap. Second, to maximize data efficiency, the framework incorporates a lightweight **Control-Adapter**, enabling state-of-the-art performance through fine-tuning on only a **limited-scale** synthetic dataset of 200K samples. Extensive experiments on standard CIR benchmarks (CIRR, FashionIQ, and CIRCO) demonstrate that Fusion-Diff significantly outperforms prior zero-shot approaches. We further enhance the interpretability of our model by visualizing the fused multimodal representations. Together, our work establishes an effective, efficient, and interpretable generative paradigm for ZS-CIR tasks.*

1. Introduction

Composed Image Retrieval (CIR) aims to retrieve a target image using a query composed of a reference image and a natural-language modification, enabling precise and user-controllable search beyond image-only or text-only retrieval [2, 10, 17, 24, 28, 41]. Consider a fashion designer seeking “this dress but in emerald green with long sleeves” or an interior architect searching for “this living room but with modern furniture.” Such compositional queries capture

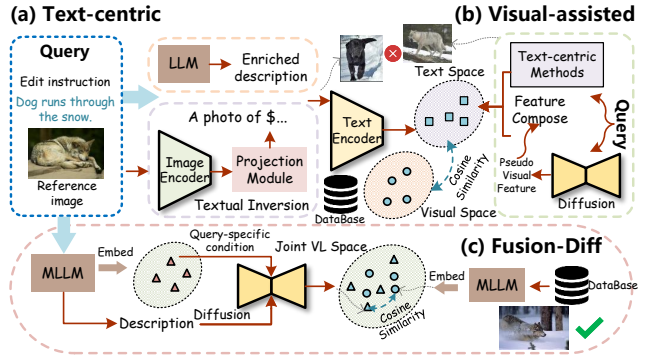


Figure 1. Comparison of different paradigms for zero-shot composed image retrieval. (a) **Text-centric methods** employ textual inversion or LLM-based description generation to perform retrieval in text space, discarding visual information. (b) **Visual-assisted methods** synthesize pseudo visual features via diffusion in visual space but still rely on text-centric retrieval mechanisms. (c) **Fusion-Diff** (Ours) operates directly in the joint vision-language space, modeling the distribution of target-fused embeddings to enable multimodal-to-multimodal retrieval, fundamentally addressing the modality gap.

how humans conceptualize visual search: building upon existing visual examples while articulating desired modifications. Despite its promise for open-world search, fashion recommendation, and e-commerce applications, CIR development has been constrained by two fundamental gaps: the *data gap*—supervised methods rely on costly triplet annotations that are difficult to generalize [11, 21]—and the *modality gap*—aligning text-image compositions to visual targets remains challenging due to inherent semantic differences between textual and visual representations.

Current Zero-Shot CIR (ZS-CIR) research has converged on several strategies to circumvent expensive triplet annotations. As illustrated in Figure 1(a), *text-centric* approaches including *inversion-based* methods [3, 36, 39] map the reference image into the text space via textual inversion, simplifying the task to text-to-image retrieval but discard-

*Equal contribution.

†Corresponding authors.

ing fine-grained visual information. *MLLM-based* methods [4, 20, 40] leverage multimodal large language models (MLLM) to generate enriched textual descriptions, yet still perform cross-modal text-to-image matching. More recently, as shown in Figure 1(b), *visual-assisted* generative approaches [26, 43] synthesize pseudo-target visual features using diffusion models in the visual space, then compose them with text-centric methods for retrieval, but noise in synthesized features can misdirect retrieval focus.

Despite their differences, all existing methods share a fundamental limitation: they ultimately perform *cross-modal* retrieval by matching text-based or text-enriched query representations against visual features, perpetuating the vision-language semantic gap. Text captures concepts through discrete symbolic representations, while visual features encode spatial, textural, and compositional information through continuous embeddings. This modality misalignment manifests as suboptimal retrieval performance, particularly for queries requiring fine-grained visual understanding. The core issue is the architectural choice to retrieve visual targets using query representations from a different modality space. This naturally inspires a pivotal question: *could we instead perform retrieval within a unified joint vision-language space under the zero-shot setting?*

To address this challenge, we propose **Fusion-Diff**, a novel framework that performs retrieval by matching multimodal-to-multimodal representations rather than text-to-visual representations, as illustrated in Figure 1(c).

However, implementing this paradigm presents two critical challenges:

- **Distribution Modeling:** How can we effectively model the conditional distribution of fused multimodal representations without ground-truth target images during training? The multimodal fusion space exhibits intricate geometric structures where visual and textual semantics interact non-linearly. Moreover, the mapping from reference-modification pairs to target embeddings is inherently one-to-many: the same inputs can correspond to multiple valid interpretations depending on compositional ambiguity. Standard diffusion conditioning mechanisms prove insufficient, struggling to disentangle modification semantics from reference structure and model the uncertainty inherent in compositional interpretation.
- **Data Efficiency:** How can we train such a diffusion model without massive-scale annotated triplet datasets, which would undermine the zero-shot advantage? Existing diffusion-based methods like CompoDiff [13] rely on billions of synthetic triplets, incurring substantial computational costs. The challenge lies in achieving strong feature editing capabilities while training on limited data, performing meaningful edits in high-dimensional multimodal feature space without overfitting or losing generalization across diverse domains.

To address the distribution modeling challenge, we introduce a conditional diffusion prior that operates directly in the joint vision-language space learned by pre-trained MLLMs. Our framework leverages an MLLM to generate target-oriented textual descriptions while producing fused embeddings from reference images and modification texts. We then learn a conditional distribution over target-fused embeddings, enabling us to sample multiple target-aware hypotheses at inference and perform ensemble retrieval in the multimodal pathway, effectively mitigating the vision-language gap while maintaining semantic consistency with both reference structure and modification instructions.

To address the data efficiency challenge, we introduce a lightweight **Control-Adapter** architecture that enables effective feature editing with minimal training data. Instead of training from scratch on billions of samples, our Control-Adapter is a parameter-efficient module that adapts a pre-trained diffusion backbone to the compositional editing task. We construct a compact synthetic dataset of only 200K triplets by mining semantically related image pairs from existing datasets and generating attribute-focused modification texts. The Control-Adapter injects compositional conditioning at multiple diffusion stages while preserving the generalization capability of the pre-trained backbone, allowing Fusion-Diff to achieve state-of-the-art performance with two orders of magnitude less training data than prior diffusion-based methods.

Our contributions are: (1) We propose the first framework to perform zero-shot composed image retrieval by modeling and sampling from the distribution of target-fused embeddings in a joint vision-language space, fundamentally addressing the modality gap. (2) We introduce a conditional diffusion prior over multimodal-fused features that captures the complex distribution of potential targets. (3) We design a lightweight Control-Adapter achieving strong feature editing with only 200K synthetic samples, demonstrating superior data efficiency. (4) Extensive experiments show that Fusion-Diff substantially outperforms existing zero-shot baselines while providing interpretable multimodal features.

2. Related Work

2.1. Zero-Shot Composed Image Retrieval

Composed Image Retrieval facilitates fine-grained image search by combining a reference image with a textual edit. While early methods relied on fully supervised training with (I_r, T_Δ, I_t) triplets, the high cost of annotating such datasets has motivated a shift towards zero-shot CIR, which does not require triplet supervision. One prominent direction is inversion-based methods [36] [3]. These approaches function by projecting the reference image into the text space, creating "pseudo-tokens" that are then combined

with the edit description. This compression of visual information into a textual format, however, struggles to retain fine-grained details. A contrasting strategy leverages Multimodal Large Language Models (MLLMs) [20] [40] [4]. Here, the MLLM reasons over the composed query to generate a completely new, rich textual description of the target, which then directs the search. Despite their architectural differences, a common limitation persists: both paradigms enrich the query primarily on the textual side, failing to incorporate explicit visual evidence of the target and thus leaving the core modality gap unaddressed.

2.2. Multimodal Fusion and Joint Vision-Language Spaces

Vision-Language (VL) representation learning has evolved significantly. Initial works, exemplified by CLIP [33] and ALIGN [19], utilized a dual-encoder, late-fusion paradigm, which cannot represent compositional concepts in a single vector. Subsequent MLLMs, from BLIP-2 [25] to PaLI-3 [9], employed deep cross-modal fusion, but their representations are optimized for *text generation*, not as explicit, retrievable embeddings. A more recent consensus, seen in works like ImageBind [12], UNIVERSAL [15], MM-EMBED [30], and GME [48], advocates for a unified joint embedding space that holistically models the static joint distribution. While these advances validate the unified space, they do not address the core CIR challenge: modeling the *semantic transformation* from a query to a target. Our Fusion-Diff is the first to propose a conditional diffusion model operating directly within this unified VL space. This allows us to perform retrieval via multimodal-to-multimodal matching, directly addressing the modality gap that plagues prior ZS-CIR methods.

2.3. Diffusion Models and Controllable Generation

Diffusion Models have become state-of-the-art in generative tasks [7, 16, 37, 45], producing high-fidelity images conditioned on various inputs. Latent diffusion models [34] made this process more efficient by operating in a compressed latent space, driving tasks from T2I synthesis [35, 47] to editing [5, 31] and personalization [35]. This generative-feedback paradigm was adopted in CIR [13, 26, 43], where pseudo-target visual information is synthesized. This two-stage approach, however, is computationally expensive and critically bottlenecks retrieval performance on generative artifacts. Our Fusion-Diff adapts diffusion for a novel task: generative modeling in joint vision-language space. We are the first in ZS-CIR to learn a conditional diffusion prior directly on the distribution of the unified joint VL space. By sampling feature hypotheses rather than pixels, we bypass pixel-space pitfalls and enable robust, multimodal matching.

3. Methodology

To resolve the modality gap identified in Sec. 1, we propose Fusion-Diff, which performs retrieval within a joint vision-language space. Our method overcomes the key challenges of distribution modeling and data efficiency via a bifurcated training strategy: (1) we pre-train a conditional diffusion prior to model the distribution of joint vision-language space, and (2) we fine-tune with a lightweight, data-efficient Control-Adapter for the compositional edit task. An overview of our architecture is depicted in Figure 2.

3.1. Joint Vision-Language Space Preliminaries

We adopt a multimodal large language model denoted by f_M that can accept images, text, or image-text pairs as input. For any input x , we first construct an instruction-augmented multimodal sequence and feed it into f_M to obtain a sequence of hidden states. Inspired by previous research [27, 42, 48], we use the final hidden state of the last token followed by ℓ_2 normalization to obtain embeddings $z(x) \in \mathbb{R}^d$ in a shared joint vision-language embedding space $\mathcal{Z} \subset \mathbb{R}^d$.

3.2. Stage 1: Pre-training the Diffusion Prior over the Joint Vision-Language Space

The goal of the first stage is to learn a diffusion prior over fused multimodal representations in the joint vision-language space \mathcal{Z} . We train on a large-scale corpus of generic image-text pairs $\mathcal{D}_{\text{pair}} = \{(I_i, T_i)\}$, where each pair is mapped to a fused multimodal representation $z_0 \in \mathbb{R}^d$ by the MLLM f_M . Specifically, for a pair $(I, T) \in \mathcal{D}_{\text{pair}}$, we construct an instruction-augmented multimodal input $x_{\text{pair}} = (I, T)$ and obtain

$$z_0 = f_M(x_{\text{pair}}), \quad (1)$$

so that z_0 lies on the manifold of valid joint vision-language embeddings in \mathcal{Z} and serves as the clean sample for diffusion.

We follow the standard DDPM formulation and apply a forward noising process to z_0 . At timestep $n \in \{1, \dots, N\}$, a noisy fused feature is obtained in closed form as

$$z_n = \sqrt{\bar{\alpha}_n} z_0 + \sqrt{1 - \bar{\alpha}_n} \epsilon, \quad (2)$$

where $\epsilon \sim \mathcal{N}(0, \mathbf{I})$ and $\bar{\alpha}_n = \prod_{s=1}^n (1 - \beta_s)$ is defined by a fixed variance schedule $\{\beta_s\}_{s=1}^N$. The diffusion model is then trained to predict the added noise from the noisy feature z_n , the timestep n , and a textual condition derived from the paired description.

Pre-training Objective. For conditioning, we encode the text T with a frozen text encoder $\mathcal{E}_{\text{text}}$ to obtain $c_T =$

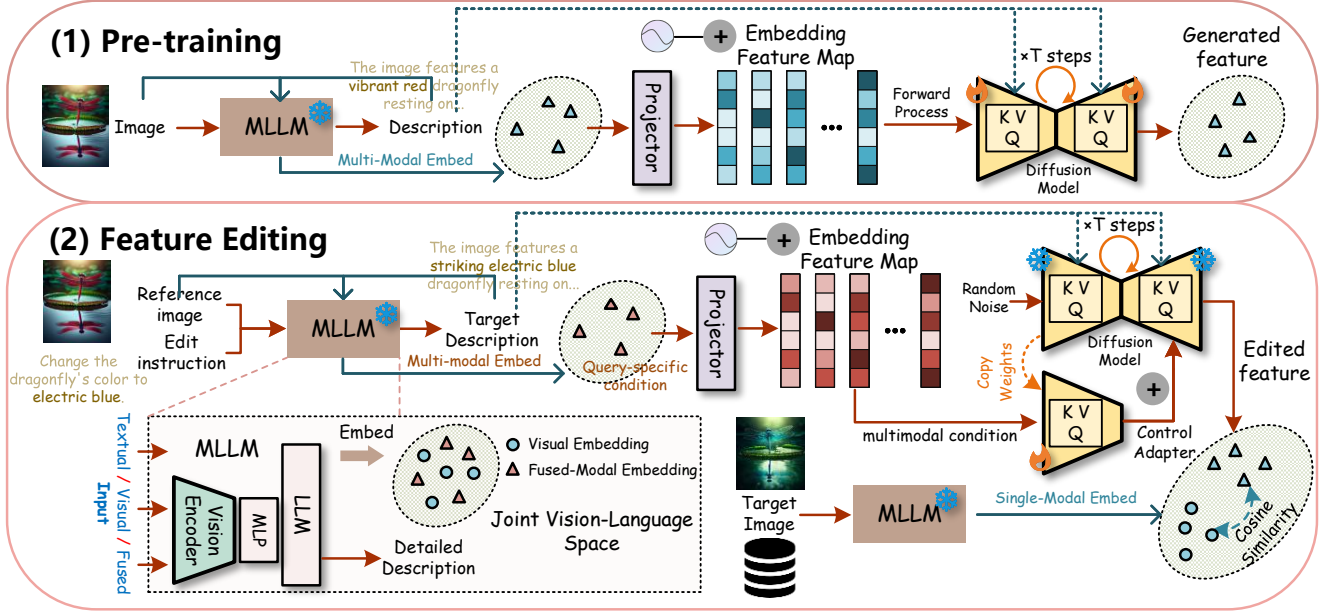


Figure 2. The Framework of Fusion-Diff.

$\mathcal{E}_{\text{text}}(T)$. The denoising network ϵ_θ receives (z_n, n, c_T) and is optimized with an ℓ_2 noise-prediction loss:

$$\mathcal{L}_{\text{Stage1}} = \mathbb{E}_{(I, T) \sim \mathcal{D}_{\text{pair}}, \epsilon, n} \left[\left\| \epsilon - \epsilon_\theta(z_n, n, c_T) \right\|_2^2 \right]. \quad (3)$$

Through this stage, ϵ_θ learns a text-conditioned diffusion prior over the manifold of joint vision-language embeddings $z(x) \in \mathcal{Z}$ produced by f_M from generic image-text pairs.

Classifier-Free Guidance. At sampling time, we adopt classifier-free guidance (CFG) to balance diversity and text fidelity. During pre-training, the text condition is randomly dropped with probability p_{cfg} to learn unconditional and conditional branches in one network. At inference, we combine the two noise predictions with guidance scale γ :

$$\tilde{\epsilon}_\theta(z_n, n, c_T) = (1 + \gamma) \epsilon_\theta(z_n, n, c_T) - \gamma \epsilon_\theta(z_n, n, \emptyset). \quad (4)$$

3.3. Stage 2: Feature Editing over the Joint Vision-Language Space using Control-Adapter

The second stage adapts the pretrained diffusion model to composed image retrieval by editing features directly in the joint vision-language space \mathcal{Z} . We fine-tune on triplets (I_r, T_Δ, I_t) , where I_r is the reference image, T_Δ is the edit instruction, I_t is the target image, and T_t is the associated target description from the dataset.

For each triplet, we form two embeddings in \mathcal{Z} using the MLLM f_M . The query-specific feature is obtained from the composed input $x_q = (I_r, T_\Delta)$ as

$$z_{r, \Delta} = z(x_q) = f_M(x_q) \in \mathbb{R}^d,$$

and the target feature is obtained from $x_t = (I_t, T_t)$ as

$$z_t = z(x_t) = f_M(x_t) \in \mathbb{R}^d.$$

Together with the text condition c_Δ , $z_{r, \Delta}$ provides query-specific conditioning and z_t provides target-side supervision for diffusion-based feature editing in \mathcal{Z} .

Fine-tuning Objective. The fine-tuning objective is to train the denoiser ϵ_θ to reconstruct z_t from its noised version, conditioned on both the composed reference feature $z_{r, \Delta}$ and the edit text T_Δ . Let $c_\Delta = \mathcal{E}_{\text{text}}(T_\Delta)$ be the embedding of the edit text. The fine-tuning loss is formulated as:

$$\mathcal{L}_{\text{Stage2}} = \mathbb{E}_{(I_r, T_\Delta, I_t), \epsilon, n} \left[\left\| \epsilon - \epsilon_\theta(z_n, n, z_{r, \Delta}, c_\Delta) \right\|_2^2 \right], \quad (5)$$

Control-Adapter for query-specific conditioning Let ϵ_θ denote the denoising network operating in \mathcal{Z} , whose encoder is composed of L blocks $\{F_l(\cdot; \Theta_l)\}_{l=1}^L$. To enable precise conditioning on the query-specific feature while preserving the original generative prior, we introduce a Control-Adapter branch that augments each block with a trainable copy and zero-initialized linear layers. For each DiT encoder block $F(\cdot; \Theta)$, we instantiate a control block $F_c(\cdot; \Theta_c)$ initialized from Θ , together with two types of zero linear layers $Z_1(\cdot; \Theta_{z1})$ and $Z_2(\cdot; \Theta_{z2})$.

Denote by h_{l-1}^{enc} the input to the l -th DiT encoder block and by $h_{c, l-1}^{\text{enc}}$ the input to the l -th control block. For the output of the Control-Adapter $y_c =$

$\{\mathbf{y}_{c,1}, \mathbf{y}_{c,2}, \dots, \mathbf{y}_{c,l}, \dots, \mathbf{y}_{c,L}\}$, where $\mathbf{y}_{c,l}$ is the l -th block output of Control Adapter, which becomes the input for the $(L - l + 1)$ -th decoder block of DiT:

$$\mathbf{y}_{c,l} = F(\mathbf{h}_{l-1}^{enc}; \Theta_l) + Z_2(F_c(\mathbf{h}_{c,l-1}^{enc}; \Theta_{c,l}); \Theta_{z2,l}) \quad (6)$$

where $\mathbf{h}_{c,l-1}^{enc} = \mathbf{h}_{l-1}^{enc} + Z_1(z_{r,\Delta}; \Theta_{z1})$ for $l = 1$, and $\mathbf{h}_{c,l-1}^{enc} = \mathbf{y}_{c,l-1}$ for $l > 1$. Both Z_1 and Z_2 are initialized with zero weights and biases. At the beginning of training, their outputs are exactly zero, so that $\mathbf{y}_{c,l} = F(\mathbf{h}_{l-1}^{enc}; \Theta_l)$ and the Control-Adapter does not perturb the original denoising behavior. As training proceeds, the control branch gradually learns how to modulate intermediate features using $z_{r,\Delta}$, while the DiT parameters remain frozen.

For the decoder, we inject the control signal by residual addition. Let $\tilde{\mathbf{h}}_l^{dec}$ denote the output of the l -th decoder block. We feed $\tilde{\mathbf{h}}_l^{dec} + \delta \mathbf{y}_{c,L-l}$ into the $(l + 1)$ -th decoder block, while the parameters of DiT encoder and decoder remain frozen. In this way, the pretrained model provides a strong generative prior, and the Control-Adapter learns a lightweight, query-conditioned residual that steers the feature editing process in \mathcal{Z} without causing catastrophic forgetting.

3.4. Inference and Retrieval

Query and Condition Generation. At inference time, given a composed query (I_r, T_Δ) , we first compute its fused representation and the corresponding textual condition in the joint vision-language space \mathcal{Z} . The query-specific embedding is obtained from the multimodal input

$$x_q = (I_r, T_\Delta), \quad z_{r,\Delta} = z(x_q) = f_M(x_q) \in \mathbb{R}^d.$$

To provide richer textual guidance than the raw edit instruction, we further use the same MLLM f_M to infer a detailed target-oriented description from the query. Specifically, we construct an instruction-augmented input

$$x_{\text{cond}} = ([\text{INST}], I_r, T_\Delta),$$

where $[\text{INST}]$ denotes a textual instruction for describing the desired target, and obtain $\tilde{T} = f_M(x_{\text{cond}})$. The inferred description is then encoded by the frozen text encoder to produce $c_{\tilde{T}} = \mathcal{E}_{\text{text}}(\tilde{T})$.

Target Feature Sampling. We then run the learned reverse diffusion process in \mathcal{Z} to generate a single target feature hypothesis. Starting from an initial noise vector $\hat{z}_N \sim \mathcal{N}(0, \mathbf{I})$, we iteratively denoise for timesteps $n = N, \dots, 1$ using the denoiser ϵ_θ :

$$\hat{z}_{n-1} = \frac{1}{\sqrt{\alpha_n}} \left(\hat{z}_n - \frac{1 - \alpha_n}{\sqrt{1 - \alpha_n}} \epsilon_\theta(\hat{z}_n, n, z_{r,\Delta}, c_{\tilde{T}}) \right) + \sigma_n \mathbf{w}_n, \quad (7)$$

where $\mathbf{w}_n \sim \mathcal{N}(0, \mathbf{I})$ and σ_n is the noise standard deviation at timestep n . After N steps, we obtain the final target feature hypothesis $\hat{z}_0 = \hat{z}_0 \in \mathcal{Z}$.

Retrieval and Ranking. For retrieval, each gallery image I_g in the database $\mathcal{D}_{\text{gallery}}$ is embedded into the same joint space using the MLLM f_M :

$$z_g = f_M(I_g) \in \mathbb{R}^d.$$

The relevance score $s(I_g)$ for I_g is computed as the cosine similarity between \hat{z}_t and z_g :

$$s(I_g) = \frac{\hat{z}_t^\top z_g}{\|\hat{z}_t\|_2 \|z_g\|_2}. \quad (8)$$

Gallery images are ranked according to $s(I_g)$, and the top-ranked ones are returned as retrieval results. Since both the generated target feature \hat{z}_t and the gallery embeddings z_g reside in the shared joint vision-language space \mathcal{Z} , retrieval is conducted entirely in a unified representation space while leveraging rich target-oriented textual guidance at inference time.

4. Experiments

In this section We conduct extensive experiments to systematically evaluate our proposed Fusion-Diff framework and validate its effectiveness in addressing the core challenges of Zero-Shot Composed Image Retrieval (ZS-CIR).

4.1. Experimental Settings

Datasets and Baselines. We evaluate Fusion-Diff on three standard ZS-CIR benchmarks and an additional real-world dataset introduced in this work, comparing with several state-of-the-art methods. CIRR [28] is built from real-life images which contains 21,552 images organized into groups of semantically related scenes and triplets (reference, textual modification, target). FashionIQ [44] is a fashion retrieval benchmark containing 77,684 images of clothing items from three categories (Dress, Shirt, Toptee) and 30,134 triplets. CIRCO [3] is a compositional retrieval benchmark on MS-COCO, featuring natural-language instructions about fine-grained attribute, layout, and content changes, with 1,020 test queries, 4,624 annotated target images, and a fixed COCO image gallery. We compare Fusion-Diff against representative state-of-the-art ZS-CIR methods, including Pic2Word [36], SEARLE [3] and LinCIR [14] under CLIP backbone ViT-G. We further include training-free LLM/MLLM reasoning approaches (CIRRevL [20], LDRE [46], OSrCIR [40]) and generative baselines (CIG [43], IP-CIR [26]).

Evaluation Metrics. For CIRR, we follow the original benchmark protocol and report Recall@ k as the primary metric, where $k \in \{1, 5, 10, 50\}$. We further evaluate performance in the subset setting using RecallSubset@ k with $k \in \{1, 2, 3\}$. On FashionIQ, we similarly adopt Recall@ k

for evaluation, with $k \in \{10, 50\}$. For CIRCO, since each query is associated with multiple target images, we use mean Average Precision at rank k (mAP@ k), where $k \in \{5, 10, 25, 50\}$ denotes the size of the top-ranked retrieval list.

Implementation Details. We implement our framework in PyTorch, training on 8 NVIDIA A100 GPUs. We adopt a T5 encoder for text processing and Qwen2.5VL-72B-Instruct [1] as the MLLM f_M . Further details on the model architecture and hyperparameters are available in the Appendix.

4.2. Quantitative Results on ZS-CIR Benchmarks

CIRCO. We present the experimental results on the CIRCO test dataset in the left half of Table 1. Across all four cutoffs, Fusion-Diff attains the best mAP@ k (e.g., 40.37 at $k=50$), improving over the strongest prior baseline (*LDRE+IP-CIR*) by +2.34 absolute at mAP@50 (+6.1%), +2.31 at mAP@25, +2.32 at mAP@10, and +2.51 at mAP@5. These gains hold against both training-free reasoning (CIReVL/LDRE/OSrCIR) and generative pipelines (LinCIR+CIG/IP-CIR, CompoDiff), indicating that editing fused features via diffusion is more robust than caption-only reasoning or pixel-space pseudo-targets on the compositional COCO benchmark.

CIRR. We present the experimental results on the CIRR test dataset in the right half of Table 1. On global retrieval, Fusion-Diff establishes new state of the art at all k (e.g., R@1=40.00, R@10=81.28), surpassing LDRE+IP-CIR by +0.75 at R@1, +1.28 at R@10, and +0.44 at R@50. On group-based evaluation, our method is *best* on R_{subset}@2/@3 and *second* on R_{subset}@1 (69.83 vs. 69.95 for LDRE+IP-CIR), narrowing the gap to the strongest one-stage CoT pipeline (OSrCIR) while outperforming two-stage reasoning (CIReVL). The pattern supports our design choice of operating directly in the joint vision–language space rather than relying solely on language-side edits.

FashionIQ. In Table 2, Fusion-Diff achieves the best results on all three categories and both metrics. For the averaged score, we obtain R@10=46.89 and R@50=67.92, improving over the strongest prior systems (LinCIR variants with/without generative auxiliaries) by +0.97 and +1.58 absolute, respectively (Table 2). Per-category gains are consistent—e.g., on *Dress* our method reaches 41.15/63.76 at R@10/R@50 (vs. 39.71/61.03 for LinCIR+CIG/IP-CIR), and on *Shirt* we set new highs at 48.23/68.45. These results indicate that our diffusion-based feature editing preserves fine-grained garment identity while applying attribute changes more faithfully than caption-only reasoning or textual-inversion baselines.

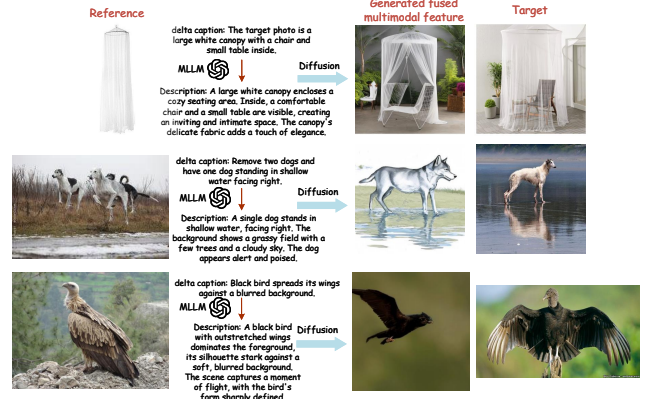


Figure 3. Visualization results on CIRR test set.



Figure 4. Visualization results on FashionIQ validation set.

4.3. Visualization of Joint Multimodal Features

To validate the effectiveness and interpretability of our method, we fine-tuned a decoder based on SANA 1.5 [45] to reconstruct images from the generated multimodal features for retrieval. Figure 3 shows the visualization results on CIRR. We observe that our method successfully interprets challenging compositional modifications, retrieving targets that require both preserving the reference image’s core identity and accurately applying fine-grained semantic edits. Similarly, Figure 4 demonstrates our model’s precision on FashionIQ, adeptly handling attribute-specific edits (e.g., color, texture, or sleeve length). These results validate our framework’s ability to perform effective retrieval in the joint multimodal space, overcoming the modality gap seen in prior cross-modal methods.

4.4. Ablation Studies

We conduct controlled ablations on FashionIQ and CIRCO to disentangle and validate the contributions of our core components, as shown in Table 3. We analyze three main

Table 1. **Comparison on CIRCO and CIRR Test Data.** Bold and underline denote the best and second-best, respectively.

CIRCO + CIRR →		CIRCO				CIRR						
		mAP@k				Recall@k			Recall _{subset} @k			
Backbone	Method	k=5	k=10	k=25	k=50	k=1	k=5	k=10	k=50	k=1	k=2	k=3
ViT-B/32	Image-only	1.34	1.60	2.12	2.41	6.89	22.99	33.68	59.23	21.04	41.04	60.31
	Text-only	2.56	2.67	2.98	3.18	21.81	45.22	57.42	81.01	62.24	81.13	90.70
	Image + Text	2.65	3.25	4.14	4.54	11.71	35.06	48.94	77.49	32.77	56.89	74.96
ViT-L/14	Pic2Word	8.72	9.51	10.64	11.29	23.90	51.70	65.30	87.80	53.76	74.46	87.07
	SEARLE-XL	11.68	12.73	14.33	15.12	24.24	52.48	66.29	88.84	53.76	75.01	88.19
ViT-G/14	LinCIR	19.71	21.01	23.13	24.18	35.25	64.72	76.05	-	63.35	82.22	91.98
	LinCIR + CIG-XL	20.64	21.90	24.04	25.20	34.43	64.51	76.12	93.54	62.24	81.35	91.28
	LinCIR + IP-CIR	25.70	26.64	29.09	30.13	35.37	64.70	76.15	93.71	62.58	81.74	91.35
	CompoDiff	15.33	17.71	19.45	21.01	26.71	55.14	74.52	92.01	64.54	82.39	91.81
	CIReVL	26.77	27.59	29.96	31.03	34.65	64.29	75.06	91.66	67.95	84.87	93.21
	LDRE	31.12	32.24	34.95	36.03	36.15	66.39	77.25	93.95	68.82	85.66	93.76
	LDRE + IP-CIR	32.75	34.26	36.86	38.03	39.25	70.07	80.00	94.89	69.95	86.87	94.22
	OSrCIR	30.47	31.14	35.03	36.59	37.26	67.25	77.33	-	69.22	85.28	93.55
		35.26	36.58	39.17	40.37	40.00	70.27	81.28	95.33	69.83	86.90	94.24

Table 2. **Comparison on FashionIQ Validation Data.** Bold and underline denote the best and second-best, respectively.

Fashion-IQ →		Shirt		Dress		Toptee		Average	
		R@10	R@50	R@10	R@50	R@10	R@50	R@10	R@50
ViT-B/32	Image-only	6.92	14.23	4.46	12.19	6.32	13.77	5.90	13.37
	Text-only	19.87	34.99	15.42	35.05	20.81	40.49	18.70	36.84
	Image + Text	13.44	26.25	13.83	30.88	17.08	31.67	14.78	29.60
ViT-L/14	Pic2Word	26.20	43.60	20.00	40.20	27.90	47.40	24.70	43.70
	SEARLE	26.89	45.58	20.48	43.13	29.32	49.97	25.56	46.23
ViT-G/14	LinCIR	46.76	65.11	38.08	60.88	50.48	71.09	45.11	65.69
	LinCIR + CIG-XL	47.35	<u>66.68</u>	<u>39.71</u>	60.93	<u>50.69</u>	<u>71.39</u>	<u>45.92</u>	<u>66.34</u>
	LinCIR + IP-CIR	<u>48.04</u>	<u>66.68</u>	39.02	<u>61.03</u>	50.18	71.14	45.74	66.28
	CompoDiff	41.31	55.17	37.78	49.10	44.26	56.41	39.02	51.71
	CIReVL	34.01	51.92	27.56	50.04	36.29	56.63	32.62	52.86
	LDRE	35.94	58.58	26.11	51.12	35.42	56.67	32.49	55.46
	OSrCIR	38.65	54.71	33.02	54.78	41.04	61.83	37.57	57.11
	Fusion-Diff	48.23	68.45	41.15	63.76	51.30	71.55	46.89	67.92

variants: (A) a baseline using only the fused feature without diffusion, (B) a diffusion model conditioned *only* on text, and (C) our complete Fusion-Diff framework.

Settings. **(A) $z_{r,\Delta}$ -only retrieval (no diffusion).** Given a composed query (I_r, T_Δ) , we embed it once to obtain $z_{r,\Delta}$ and rank gallery items by cosine similarity $s(I_g) =$

$\langle z_{r,\Delta}, z_g \rangle$, with no diffusion sampling or editing. This baseline quantifies how far a strong fused representation can go without any generative refinement.

(B) Stage-I-only (text-conditioned prior). We use only the pretrained text-conditioned diffusion prior from Stage I to generate a single target feature hypothesis \hat{z}_t *without* Stage II editing. Concretely, we drop $z_{r,\Delta}$ and condition the

Table 3. Ablations on FashionIQ and CIRCO. (A) $z_{r,\Delta}$ -only: Uses the fused feature with no diffusion. (B) Stage-I-only: Uses text-conditioned diffusion prior *without* image-aware control. (C) Full Model (Fusion-Diff): Uses the full pipeline with *both* the Control-Adapter and text-side conditioning.

Variant	FashionIQ (Avg.) \uparrow		CIRCO \uparrow			
	R@10	R@50	mAP@5	mAP@10	mAP@25	mAP@50
(A) $z_{r,\Delta}$ -only (no diffusion)	40.57	61.22	14.91	16.44	18.57	19.50
(B) Stage-I-only (text-conditioned prior)	33.12	54.08	13.02	14.16	16.62	17.87
(C) Full Model (Fusion-Diff)	46.89	67.92	35.26	36.58	39.17	40.37

Avg. denotes the arithmetic mean over the three FashionIQ categories (Dress, Shirt, Toptee).

reverse process with the text side only (using the MLLM-inferred \tilde{T}) to obtain \hat{z}_t , which is then used for retrieval. This isolates the effect of a generic text-to-feature generative prior.

(C) Full Model (Fusion-Diff). This is our full proposed framework, which executes Stage II feature editing using both the text-side conditioning (driven by \tilde{T}) and the image-aware Control-Adapter (driven by $z_{r,\Delta}$). This variant matches the main results reported in Tables 1 and 2.

Discussion. The results in Table 3 validate our design:

- **Necessity of Diffusion Refinement.** Variant (A) ($z_{r,\Delta}$ -only) establishes a strong baseline (e.g., 40.57 R@10 on FashionIQ), indicating a high-quality initial query embedding. However, our Full Model (C) dramatically improves upon this (46.89 R@10), proving that the generative refinement provided by our diffusion process is crucial for achieving top-tier performance.
- **Necessity of Control-Adapter.** Variant (B) (text-only diffusion) performs very poorly (33.12 R@10 on FashionIQ, 13.02 mAP@5 on CIRCO), scoring significantly *worse* than the non-diffusion baseline (A). This highlights a critical failure mode: text-conditioning alone is insufficient and fails to preserve the reference image’s core visual identity.
- **Synergy of Dual-Conditioning.** Our Full Model (C) succeeds by combining both pathways. By comparing (C) against (A) and (B), we conclude that *both* components are essential. The Control-Adapter (missing in B) is vital for preserving visual identity, while the text-conditioning (analyzed in Sec. 4.5) is vital for guiding the feature towards the correct semantic edit. This dual-conditioning synergy is the key to our state-of-the-art results.

4.5. Parameter Sensitivity Analysis

We study the sensitivity of three key hyperparameters, with results shown in Figure 5: the text-guidance scale γ and Control-Adapter strength δ (analyzed on CIRR R@10), and the number of denoising steps N (analyzed on FashionIQ Avg. R@50).

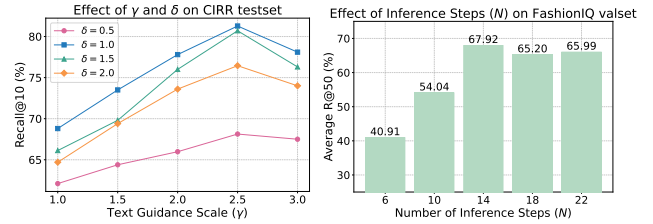


Figure 5. Parameter sensitivity analysis on CIRR test set and FashionIQ validation set.

Effect of γ and δ . As shown in Figure 5 (left), performance is sensitive to the balance between text guidance (γ) and visual control (δ). We observe a clear peak at ($\gamma = 2.5, \delta = 1.0$), achieving 81.28% R@10 on CIRR. Performance degrades if either guidance is too weak (e.g., $\delta = 0.5$) or too strong (e.g., $\gamma > 2.5$), confirming the need for a balanced interplay to apply the edit without overriding the reference image.

Effect of N . Figure 5 (right) shows the impact of denoising steps N on FashionIQ Avg. R@50. Performance is poor with too few steps (40.91% at $N = 6$) but rises sharply to a peak of 67.92% at $N = 14$. Beyond this, returns diminish and performance slightly degrades (e.g., at $N = 18, 22$) while latency increases. We thus select $N = 14$ as the optimal accuracy–efficiency trade-off.

5. Conclusion and Limitations

We propose Fusion-Diff, a novel generative framework that reframes zero-shot composed image retrieval (ZS-CIR) as multimodal-to-multimodal matching. Our Control-Adapter architecture mitigates data inefficiency through lightweight, parameter-efficient fine-tuning, while the joint vision-language space representation bridges the modality gap. Experiments on CIRR, FashionIQ, and CIRCO demonstrate superior performance over existing methods. Nevertheless, standard diffusion sampling introduces additional computational overhead; future work will explore acceleration techniques.

Generative Editing in the Joint Vision-Language Space for Zero-Shot Composed Image Retrieval

Supplementary Material

6. Zero-Shot Protocol and Data Settings

In all experiments, we strictly adhere to the zero-shot composed image retrieval (ZS-CIR) protocol. Our model is never trained on any triplets, images, or annotations from the evaluation benchmarks (CIRR [28], FashionIQ [44], and CIRCO [3]). All training data are derived from public datasets with domains disjoint from the test sets, ensuring that evaluation images and captions remain completely unseen during the training phase.

6.1. VL Diffusion Prior Pre-Training

To learn a robust generative prior, we construct a large-scale corpus, $\mathcal{D}_{\text{pair}}$, comprising 33 million image-text pairs collected from public datasets distinct from the downstream benchmarks. Following the data construction recipe of BLIP3-o [8], we aggregate images from open-source datasets including CC12M [6], SA-1B [23], and JourneyDB [38]. To ensure the model generalizes across varying text granularities, we implement a mixed-length captioning strategy:

- **Long-Text Subset (28M):** To ensure semantically rich supervision, this subset comprises detailed synthetic captions generated by Qwen2.5-VL-7B-Instruct [1], with an average length of approximately 120 tokens.
- **Short-Text Subset (5M):** To mitigate overfitting to verbose descriptions and maintain alignment with concise queries, this subset consists of original short captions (avg. 20 tokens) sourced from the CC12M dataset.

For every pair $(I, T) \in \mathcal{D}_{\text{pair}}$, we feed the image and text into the frozen MLLM f_M to obtain a fused vision-language (VL) representation $z_0 = f_M(I, T)$ within the joint embedding space. Stage 1 trains the text-conditioned diffusion model to estimate the distribution of these fused features. This pre-training strategy offers three key advantages:

1. **Geometric Alignment:** It aligns the diffusion prior with the intrinsic geometry of the joint VL space used for retrieval.
2. **Robustness:** It enhances robustness to varying text lengths and styles, as the model is exposed to a diverse range of caption distributions (from the 28M detailed descriptions to the 5M concise captions).
3. **Generalization:** It establishes a generic, dataset-agnostic prior that facilitates effective transfer to the composed image retrieval task using limited synthetic data.

6.2. Synthetic Editing Alignment

In the second stage, we leverage the HQEdit dataset [18] to instill query-dependent editing capabilities into the joint VL space via the Control-Adapter. HQEdit contains approximately 200K synthetic triplets (I_r, T_Δ, I_t) , generated to provide high-quality instruction-following examples while remaining disjoint from real-world CIR benchmarks. This stage fine-tunes the Control-Adapter to modulate the pre-trained prior based on the reference image I_r and edit instruction T_Δ .

6.3. Inference-Time Target Description Generation

During inference, our framework requires a detailed textual description of the target image to guide the diffusion process in the VL space. Since ground-truth target captions are unavailable in the ZS-CIR setting, we employ the MLLM f_M to hallucinate a pseudo-target description \tilde{T} based on the reference image I_r and the edit instruction T_Δ .

We construct specific instruction prompts (denoted as `INST`) for each benchmark to optimize the MLLM’s generation quality. The prompts are formulated as follows:

To optimize the MLLM’s generation quality and ensure semantic consistency across all benchmarks (CIRCO, CIRR, and FashionIQ), we adopt a unified instruction template. This template explicitly enforces a constraint to preserve the core visual identity while applying the modification. The prompt is formulated as follows:

“<image> Change the image into a new one according to the requirement of the editing prompt ‘{ T_Δ }’ with a shared concept ‘{shared_concept}’ remaining unchanged. Objectively describe the new image after editing.”

In this template, the shared concept is instantiated with the coarse category of the reference image (e.g., “dog” for CIRR or “dress” for FashionIQ) to anchor the MLLM’s reasoning. The generated description \tilde{T} is then embedded and used alongside the reference image I_r to sample the final target feature z_t via the diffusion prior.

7. Implementation Details of Fusion-Diff

Network Architecture of the Diffusion Prior

We formulate the diffusion prior as a conditional Diffusion Transformer (DiT) [32] operating directly within the joint vision-language (VL) manifold. Let f_M denote the

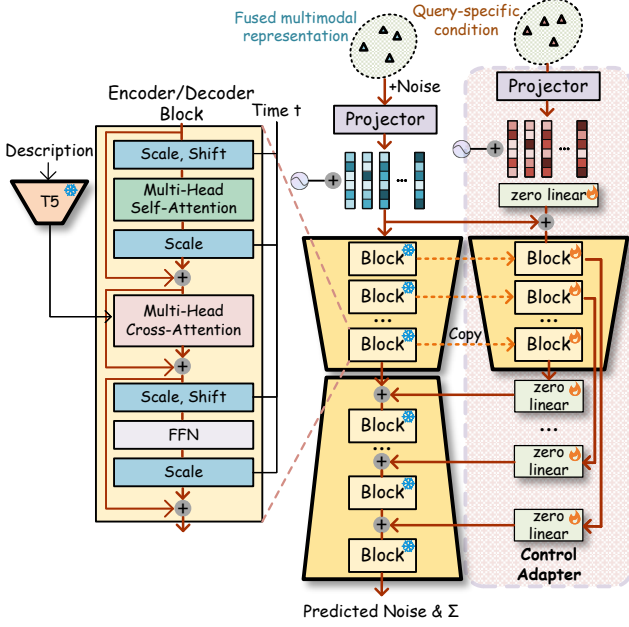


Figure 6. Architecture of the Fusion-Diff Diffusion Prior. The model processes fused VL embeddings as pseudo-spatial feature maps, modulated by timestep and text conditions via a transformer backbone.

MLLM. For an input image–text pair, f_M yields a fused representation $z_0 \in \mathbb{R}^{d_{VL}}$, where $d_{VL} = 1536$. We model $z_0 \sim p_{\text{data}}(z_0)$ as the data variable, eschewing pixel-space decoding or VAE latent compression. The overall architecture is illustrated in Figure 6.

Forward Process and Feature Projection. We adopt the standard Gaussian diffusion formulation [16]. The forward process $q(z_n|z_0)$ imposes noise according to a variance schedule $\{\beta_n\}_{n=1}^N$:

$$z_n = \sqrt{\bar{\alpha}_n} z_0 + \sqrt{1 - \bar{\alpha}_n} \epsilon, \quad \epsilon \sim \mathcal{N}(0, \mathbf{I}), \quad (9)$$

where $\alpha_n = 1 - \beta_n$ and $\bar{\alpha}_n = \prod_{s=1}^n \alpha_s$. To leverage the inductive biases of vision transformers, we project the unstructured vector z_n into a pseudo-spatial feature map. We define a learnable linear projector $\mathcal{P} : \mathbb{R}^{d_{VL}} \rightarrow \mathbb{R}^{C \times H \times W}$ with $(C, H, W) = (4, 32, 32)$, such that:

$$\mathbf{H}_n = \mathcal{P}(z_n) \in \mathbb{R}^{4 \times 32 \times 32}. \quad (10)$$

This mapping \mathcal{P} transforms the fused VL embedding into a structured tensor \mathbf{H}_n , analogous to a latent feature map, enabling patch-based processing.

Transformer Backbone Formulation. The backbone processes \mathbf{H}_n via patchification. We partition \mathbf{H}_n into non-overlapping patches of size $p \times p$ (where $p = 2$), resulting

in a sequence of $M = (H/p)(W/p) = 256$ tokens. These are linearly projected to a hidden dimension $D = 1152$ and augmented with sinusoidal positional embeddings \mathbf{E}_{pos} :

$$\mathbf{X}_0 = \text{Linear}(\text{Patchify}(\mathbf{H}_n)) + \mathbf{E}_{\text{pos}} \in \mathbb{R}^{M \times D}. \quad (11)$$

The sequence \mathbf{X}_0 propagates through a stack of $L = 28$ transformer blocks. Each block ℓ incorporates timestep information n and textual conditions c_T .

Conditioning Mechanisms. Time Modulation: The timestep n is mapped to an embedding $\tau \in \mathbb{R}^D$. We employ Adaptive Layer Normalization (AdaLN), where τ regresses scale (γ) and shift (β) parameters to modulate normalized features:

$$\text{AdaLN}(\mathbf{X}, n) = \gamma(\tau) \odot \text{LN}(\mathbf{X}) + \beta(\tau). \quad (12)$$

Text Conditioning: The caption is encoded into a sequence $\mathbf{C}_{\text{text}} \in \mathbb{R}^{K \times D}$ via the text branch of f_M and a projection MLP. Interaction occurs via Multi-Head Cross-Attention (MHCA).

Block Architecture. The operation of the ℓ -th transformer block is defined by the composition of Multi-Head Self-Attention (MHSA), MHCA, and a Feed-Forward Network (FFN):

$$\mathbf{X}'_{\ell} = \mathbf{X}_{\ell-1} + \text{MHSA}(\text{AdaLN}(\mathbf{X}_{\ell-1}, n)), \quad (13)$$

$$\mathbf{X}''_{\ell} = \mathbf{X}'_{\ell} + \text{MHCA}(\text{AdaLN}(\mathbf{X}'_{\ell}, n), c_T), \quad (14)$$

$$\mathbf{X}_{\ell} = \mathbf{X}''_{\ell} + \text{FFN}(\text{AdaLN}(\mathbf{X}''_{\ell}, n)). \quad (15)$$

To balance efficiency and receptive field, we alternate MHSA between global attention and local windowed attention (window size 16×16). Zero-initialized gating is applied to the residual branches of each sub-layer for stable training dynamics.

Output Parameterization. The final hidden states \mathbf{X}_L are reshaped via a linear unpatchify operation \mathcal{P}^{-1} to recover the VL dimensionality. The network predicts the noise component ϵ_{θ} :

$$\epsilon_{\theta}(z_n, n, c_T) = \text{Linear}_{\text{out}}(\mathcal{P}^{-1}(\mathbf{X}_L)) \in \mathbb{R}^{d_{VL}}. \quad (16)$$

The model is optimized to minimize the simple diffusion objective $\|\epsilon - \epsilon_{\theta}(z_n, n, c_T)\|^2$ directly in the joint embedding space.

7.1. Training Strategy and Hyperparameters

Diffusion Prior Pre-training. We instantiate the diffusion backbone using the DiT-XL/2 architecture configuration. To adapt the model for global vision–language feature

modeling, we disable local windowed attention and relative positional encodings. Furthermore, we enforce full-precision attention computation to ensure numerical precision during the diffusion process. The model is optimized using AdamW [22] with a global batch size of 4096. We employ the following hyperparameter settings:

- Learning rate: $\eta = 2 \times 10^{-5}$;
- Weight decay: $\lambda = 3 \times 10^{-2}$;
- Optimizer stability term: $\varepsilon = 10^{-10}$.

To stabilize training dynamics under this large effective batch size, we apply global gradient clipping with an ℓ_2 -norm threshold of 0.01. The model is trained for a total of 4 epochs on the Stage 1 corpus. We utilize a learning rate warmup strategy for the initial 1000 optimization steps, followed by a cosine annealing schedule for the remainder of the training process.

Feature Editing Fine-tuning. In the second stage, we freeze the parameters of the pre-trained diffusion backbone to preserve the robust generative prior learned from large-scale pre-training. We instantiate the Control-Adapter by duplicating the weights of the DiT encoder blocks. To ensure a stable optimization start, the zero-convolution layers (linear projections connecting the adapter to the backbone) are initialized with zeros, ensuring the initial forward pass remains identical to the pre-trained prior. The model is fine-tuned on the synthetic HQEdit dataset containing approximately 200K triplets. We continue to use the AdamW optimizer [22] for fine-tuning. Given the introduction of the Control-Adapter and the reduced dataset size, we adopt the following specific settings:

- Learning rate: $\eta = 2 \times 10^{-5}$ (typically higher for adapter training);
- Weight decay: $\lambda = 2 \times 10^{-2}$;

Training is distributed across 8 NVIDIA A100 GPUs. To prevent overfitting to the synthetic edit patterns, we maintain the global gradient clipping threshold at 0.01. The Control-Adapter is trained for 2 epochs on the HQEdit dataset. We employ a constant learning rate schedule without warmup, as the Control-Adapter is initialized from pre-trained weights and the zero-initialization strategy mitigates the need for a gradual warmup phase.

8. Training Cost and Inference Speed

We provide a detailed analysis of the computational resources, training costs, and inference latency associated with Fusion-Diff. Table 4 summarizes the configuration and efficiency metrics. It is important to note that Stage 1 is a pure pre-training phase used solely to align the diffusion prior with the joint vision–language space. The actual retrieval inference is performed only after the feature editing phase, utilizing the fine-tuned Control-Adapter.

Training Efficiency. All models were trained on a node equipped with $8 \times$ NVIDIA A100 (80GB) GPUs. Pre-training is the most computationally intensive phase, requiring approximately 80 GPU-hours to align the DiT-XL/2 backbone (Total Depth $2L = 28$) using the 33M sample corpus. In contrast, Stage 2 is highly efficient; by freezing the backbone and training only the lightweight Control-Adapter on 200K synthetic triplets, we reduce the training time to approximately 0.43 GPU-hours. This demonstrates that once the generic prior is established, adapting Fusion-Diff to the composed image retrieval task is computationally inexpensive.

Accelerated Inference via DPM-Solver. During the inference phase (Stage 2), standard diffusion sampling (e.g., DDPM [16]) typically necessitates a large number of iterative denoising steps, introducing significant latency. To enable practical deployment, we employ DPM-Solver++ [29], a fast high-order solver for diffusion ODEs. Specifically, we utilize a second-order solver with a reduced number of inference steps ($N = 14$). This optimization drastically reduces the per-query inference latency to approximately 0.32 seconds (excluding MLLM encoding time) with negligible degradation in retrieval accuracy.

9. Algorithm

In this section, we present the comprehensive algorithmic framework of Fusion-Diff, encompassing four key components: (1) VL-Embed (Algorithm 1): The construction of the joint vision–language manifold using the MLLM; (2) the Stage 1 Pre-training procedure (Algorithm 2), where we learn a conditional diffusion prior over fused multimodal embeddings; (3) the Stage 2 Fine-tuning procedure (Algorithm 3), which freezes the prior and trains the Control-Adapter to perform query-specific editing; and (4) Fusion-Retrieval (Algorithm 4): the complete zero-shot inference pipeline that generates target features and ranks gallery images.

10. More Qualitative Results

To provide a more comprehensive assessment of Fusion-Diff, we present additional qualitative comparisons against two state-of-the-art zero-shot baselines: CIReVL [20] (a representative training-free, LLM-reasoning method) and LinCIR+CIG [43] (a representative generative method that synthesizes pseudo-images). We visualize the retrieval results (Recall@1) on the CIRR and FashionIQ benchmarks. These examples further substantiate our claim that modeling the conditional distribution in the joint vision–language space yields superior alignment compared to text-centric reasoning or pixel-space generation.

Table 4. Hyperparameters, training details, and compute resources for Fusion-Diff. We report metrics separately for the generic Pre-training and the task-specific Feature Editing. Note that Stage 1 is training-only; inference latency is reported only for the final model, where we utilize the DPM-Solver++ to accelerate retrieval.

Parameter / Metric	Stage 1: Pre-training	Stage 2: Feature Editing
Architecture (DiT-XL/2)		
Hidden dimension (d)	1152	1152
Attention heads	16	16
Encoder/Decoder Blocks (L)	14	14
Patch size (p)	2	2
Trainable Parameters	954M	318M
Training Configuration		
Global Batch Size	4096	1024
Optimizer	AdamW	AdamW
Learning Rate	2×10^{-5}	2×10^{-5}
Data Scale	33M (Image-Text Pairs)	200K (Synthetic Triplets)
Total Training Steps	~ 32800	~ 400
Approx. Training Time	~ 80 hours (4 epochs)	~ 26 mins (2 epochs)
Inference & Efficiency		
Status	<i>N/A (Training Only)</i>	Inference
Sampler Strategy	–	DPM-Solver++
Inference Steps (N)	–	14
Guidance Scale (γ)	–	2.5
Control Scale (δ)	–	1.0
Inference Latency (Diffusion)	–	~ 0.32 s / query

Algorithm 1 VL-Embed: Joint Vision-Language Space Construction

Require: Image-Text Pair Dataset $\mathcal{D}_{\text{pair}}$, MLLM f_M
Ensure: Latent Dataset $\mathcal{D}_{\text{latent}} = \{(z_0, c_T)\}$

- 1: $\mathcal{D}_{\text{latent}} \leftarrow \emptyset$
- 2: **for** each pair $(I, T) \in \mathcal{D}_{\text{pair}}$ **do**
- 3: **// Step 1: Construct Multimodal Input**
- 4: $x_{\text{pair}} \leftarrow \text{FormatInput}(I, T)$
- 5: **// Step 2: Extract Fused Embedding**
- 6: $z_0 \leftarrow f_M(x_{\text{pair}})$ ▷ Target fused feature in $\mathbb{R}^{d_{\text{VL}}}$
- 7: $z_0 \leftarrow \text{Normalize}(z_0)$
- 8: **// Step 3: Extract Text Condition**
- 9: $c_T \leftarrow \mathcal{E}_{\text{text}}(T)$ ▷ Caption embedding
- 10: $\mathcal{D}_{\text{latent}} \leftarrow \mathcal{D}_{\text{latent}} \cup \{(z_0, c_T)\}$
- 11: **end for**
- 12: **return** $\mathcal{D}_{\text{latent}}$

10.1. More Qualitative results on CIRR

Figure 7 illustrates qualitative results on the CIRR validation set. The queries in CIRR often involve complex spatial modifications or state changes that are difficult to capture via text alone.

Analysis of Semantic Consistency. In the first row (Wine Bottle), the query demands a specific visual view-

Algorithm 2 Stage 1: Diffusion Prior Pre-training

Require: Latent Dataset $\mathcal{D}_{\text{latent}}$, Diffusion Model ϵ_θ
Ensure: Pre-trained Parameters Θ_{prior}

- 1: Initialize Θ_{prior} randomly
- 2: **for** epoch = 1 to N_{epochs} **do**
- 3: **for** $(z_0, c_T) \in \mathcal{D}_{\text{latent}}$ **do**
- 4: $n \sim \text{Uniform}(1, N)$ ▷ Sample timestep n
- 5: $\epsilon \sim \mathcal{N}(0, \mathbf{I})$
- 6: $z_n \leftarrow \sqrt{\bar{\alpha}_n} z_0 + \sqrt{1 - \bar{\alpha}_n} \epsilon$ ▷ Eq. 2
- 7: **// Classifier-Free Guidance Training**
- 8: $u \sim \text{Uniform}(0, 1)$
- 9: **if** $u < p_{\text{cfg}}$ **then**
- 10: $c_{\text{cond}} \leftarrow \emptyset$
- 11: **else**
- 12: $c_{\text{cond}} \leftarrow c_T$
- 13: **end if**
- 14: $\epsilon_{\text{pred}} \leftarrow \epsilon_\theta(z_n, n, c_{\text{cond}})$
- 15: $\mathcal{L}_{\text{Stage1}} \leftarrow \|\epsilon - \epsilon_{\text{pred}}\|_2^2$ ▷ Eq. 3
- 16: Update Θ_{prior} using $\nabla \mathcal{L}_{\text{Stage1}}$
- 17: **end for**
- 18: **end for**

point change (“close up view of the label”). LinCIR+CIG suffers from severe hallucination, retrieving a carbonated

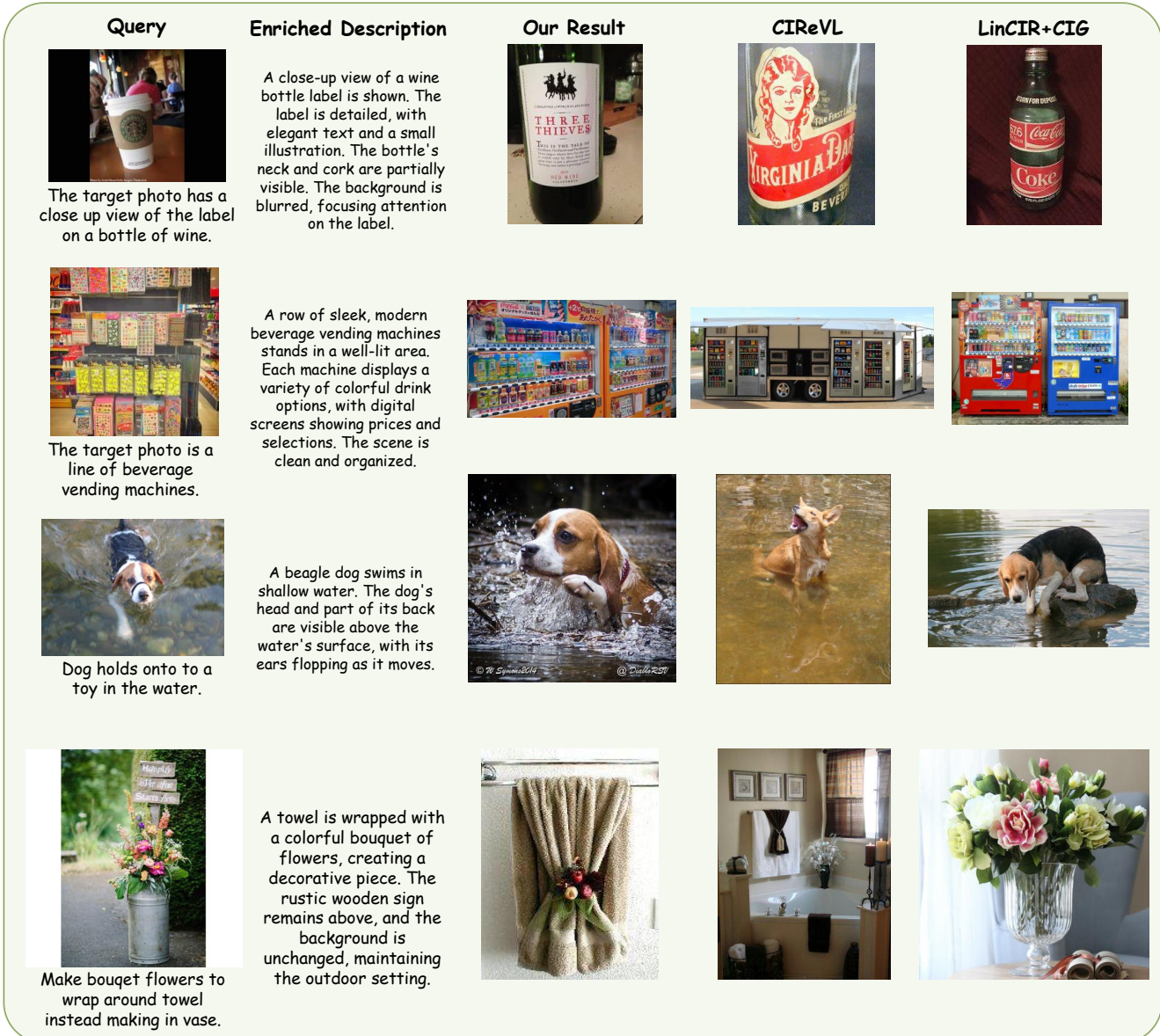


Figure 7. Additional qualitative comparison on the **CIRR** validation set. We compare the Recall@1 retrieved images of our Fusion-Diff against CIReVL [20] and LinCIR+CIG [43]. Fusion-Diff accurately captures fine-grained visual details and spatial relationships where baselines suffer from semantic drift or hallucination.

soft drink bottle which is visually distinct from the requested wine bottle category. This failure likely stems from the noise inherent in pixel-space diffusion when the textual condition (“bottle”) is broad. CIReVL, relying heavily on textual reasoning, retrieves a bottle with a completely different label structure and color palette compared to the ground truth. In contrast, Fusion-Diff successfully retrieves the correct target, demonstrating that our joint-space diffusion preserves the fine-grained visual identity and layout required by the query while faithfully executing the viewpoint change.

Analysis of Complex Composition. The fourth row (Flowers and Towel) presents a challenging compositional query: “wrap around towel instead making in vase”. CIReVL fails to capture the “wrapping” action, retrieving a standard bathroom interior. LinCIR+CIG retrieves a generic vase, ignoring the modification instruction entirely. Fusion-Diff is the only method that retrieves the correct image where the bouquet is tied around the towel. This highlights the effectiveness of the **Control-Adapter**, which injects the structural layout of the query directly into the diffusion process, enabling precise compositional reasoning that

Algorithm 3 Stage 2: Feature Editing with Control-Adapter

Require: Triplet Dataset $\mathcal{D}_{\text{edit}}$, Pre-trained Prior ϵ_θ
Ensure: Trained Control-Adapter Parameters Θ_{ctrl}

- 1: // Initialize Control-Adapter
- 2: Freeze Θ_{prior} . Initialize Θ_{ctrl} from copy/zeros.
- 3: **for** iteration = 1 to N_{iter} **do**
- 4: Sample $(I_r, T_\Delta, I_t, T_t) \sim \mathcal{D}_{\text{edit}}$
- 5: $z_{r,\Delta} \leftarrow f_M(I_r, T_\Delta)$ \triangleright Query condition
- 6: $z_t \leftarrow f_M(I_t, T_t)$ \triangleright Target Ground Truth
- 7: $c_\Delta \leftarrow \mathcal{E}_{\text{text}}(T_\Delta)$ \triangleright Text condition
- 8: $n \sim \text{Uniform}(1, N), \epsilon \sim \mathcal{N}(0, \mathbf{I})$
- 9: $z_{n,\text{noise}} \leftarrow \text{AddNoise}(z_t, n, \epsilon)$
- 10: // Control-Adapter Forward
- 11: Compute control features $\{y_c\}$ using $z_{r,\Delta}$ and $z_{n,\text{noise}}$
- 12: $\epsilon_{\text{pred}} \leftarrow \epsilon_\theta(z_{n,\text{noise}}, n, c_\Delta, \{y_c\})$
- 13: $\mathcal{L}_{\text{Stage2}} \leftarrow \|\epsilon - \epsilon_{\text{pred}}\|_2^2$ \triangleright Eq. 5
- 14: Update Θ_{ctrl} using $\nabla \mathcal{L}_{\text{Stage2}}$
- 15: **end for**

Algorithm 4 Fusion-Retrieval: Inference Pipeline

Require: Query (I_r, T_Δ) , Gallery \mathcal{D}_{gal}
Ensure: Ranked List of Images

- 1: $z_{r,\Delta} \leftarrow f_M(I_r, T_\Delta)$
- 2: $\tilde{T} \leftarrow \text{GenerateDescription}(f_M, I_r, T_\Delta)$
- 3: $c_{\tilde{T}} \leftarrow \mathcal{E}_{\text{text}}(\tilde{T})$
- 4: $\hat{z}_N \sim \mathcal{N}(0, \mathbf{I})$ \triangleright Start from noise at $n = N$
- 5: **for** $n = N$ down to 1 (or DPM steps) **do**
- 6: $\epsilon_{\text{cond}} \leftarrow \epsilon_\theta(\hat{z}_n, n, c_{\tilde{T}}, z_{r,\Delta})$
- 7: $\epsilon_{\text{uncond}} \leftarrow \epsilon_\theta(\hat{z}_n, n, \emptyset, \emptyset)$
- 8: $\tilde{\epsilon} \leftarrow (1 + \gamma)\epsilon_{\text{cond}} - \gamma\epsilon_{\text{uncond}}$ \triangleright Eq. 4
- 9: $\hat{z}_{n-1} \leftarrow \text{SolverStep}(\hat{z}_n, \tilde{\epsilon}, n)$
- 10: **end for**
- 11: // Retrieval
- 12: Calculate Cosine Similarity between \hat{z}_0 and all $z_g \in \mathcal{D}_{\text{gal}}$
- 13: **return** Top-ranked images

pure language models miss.

10.2. More Qualitative results on FashionIQ

Figure 8 showcases results on the FashionIQ validation set, focusing on fine-grained attribute manipulation (e.g., texture, pattern, and color changes).

Pattern and Symbol Alignment. The second row (Tie-dye Shirt) provides a compelling example of fine-grained pattern recognition. The edit instruction explicitly asks for a “heart in the center”. LincIR+CIG retrieves a shirt with a peace sign, illustrating a limitation where the synthesized pseudo-visual features introduce noise that misdirects the retrieval process, causing the model to capture the gen-

eral style (tie-dye) but fail to align with the specific symbol requirement. CIREVL retrieves a shirt with text (“Peace Love Softball”), failing to align with the visual concept of a “heart”. Fusion-Diff accurately retrieves the shirt featuring a heart pattern. This precision confirms that our method, by operating in the joint VL space, avoids the modality gap where text descriptions fail to fully encapsulate complex visual patterns.

Attribute and Silhouette Fidelity. In the first row (Grey Dress), the query specifies “one shoulder strap”. LinCIR+CIG retrieves a dress with a completely different silhouette (flared skirt, standard straps). CIREVL retrieves a dress that matches the “one shoulder” attribute but misses the specific texture (sequins) and fit. Fusion-Diff retrieves the exact match, preserving the tight-fitting silhouette and the metallic texture of the reference while satisfying the structural edit.

Across both datasets, comparisons reveal that Fusion-Diff significantly reduces two types of errors prevalent in baselines: (1) the hallucination of irrelevant objects seen in generative methods (LinCIR+CIG), and (2) the semantic drift seen in text-centric methods (CIREVL) where visual constraints are lost. These qualitative results strongly support the quantitative gains reported in the main paper.

Query	Enriched Description	Our Result	CIReVL	LinCIR+CIG
	Grey sequined mini dress with one shoulder strap, featuring a shimmering texture, short sleeves, and a form-fitting silhouette for a glamorous look.			
Has one shoulder strap and grey and has one shoulder strap.				
	Vibrant tie-dye shirt with swirling red, green, yellow. Central heart features intricate symbol. Tie-dye heart blends seamlessly, creating a harmonious, eye-catching design. Perfect for expressive style.			
Has a symbol and a tie dye heart and has a heart in the center.				
	Leopard print tank top featuring a bold, wild pattern. Soft, stretchy fabric for comfort. Perfect for casual wear, combining style and ease.			
The tank top is leopard print, and is a leopard print pattern.				
	Black floral dress with vibrant pink flowers, short sleeves, round neckline, and flared skirt. Similar style, elegant and feminine.			
Is blacker and more pink flowers and is very similar.				

Figure 8. Additional qualitative comparison on the **FashionIQ** validation set. Fusion-Diff demonstrates superior capability in following fine-grained attribute editing instructions (e.g., specific logos, patterns, and cuts) compared to CIReVL [20] and LinCIR+CIG [43].

References

[1] Shuai Bai, Keqin Chen, Xuejing Liu, Jialin Wang, Wenbin Ge, Sibo Song, Kai Dang, Peng Wang, Shijie Wang, Jun Tang, Humen Zhong, Yuanzhi Zhu, Ming-Hsuan Yang, Zhaohai Li, Jianqiang Wan, Pengfei Wang, Wei Ding, Zheren Fu, Yiheng Xu, Jiabo Ye, Xi Zhang, Tianbao Xie, Zesen Cheng, Hang Zhang, Zhibo Yang, Haiyang Xu, and Junyang Lin. Qwen2.5-vl technical report. *CoRR*, abs/2502.13923, 2025. 6, 9

[2] Alberto Baldrati, Marco Bertini, Tiberio Uricchio, and Alberto Del Bimbo. Effective conditioned and composed image retrieval combining clip-based features. In *IEEE/CVF Conference on Computer Vision and Pattern Recognition, CVPR 2022, New Orleans, LA, USA, June 18-24, 2022*, pages 21434–21442. IEEE, 2022. 1

[3] Alberto Baldrati, Lorenzo Agnolucci, Marco Bertini, and Alberto Del Bimbo. Zero-shot composed image retrieval with textual inversion. In *IEEE/CVF International Conference on Computer Vision, ICCV 2023, Paris, France, October 1-6, 2023*, pages 15292–15301. IEEE, 2023. 1, 2, 5, 9

[4] Tong Bao, Che Liu, Derong Xu, Zhi Zheng, and Tong Xu. MLLM-I2W: harnessing multimodal large language model for zero-shot composed image retrieval. In *Proceedings of the 31st International Conference on Computational Linguistics, COLING 2025, Abu Dhabi, UAE, January 19-24, 2025*, pages 1839–1849. Association for Computational Linguistics, 2025. 2, 3

[5] Tim Brooks, Aleksander Holynski, and Alexei A. Efros. Instructpix2pix: Learning to follow image editing instructions. In *IEEE/CVF Conference on Computer Vision and Pattern Recognition, CVPR 2023, Vancouver, BC, Canada, June 18-22, 2023*, pages 18392–18402. IEEE Computer Society, 2023. 3

[6] Soravit Changpinyo, Piyush Sharma, Nan Ding, and Radu Soricut. Conceptual 12m: Pushing web-scale image-text pre-training to recognize long-tail visual concepts. In *IEEE Conference on Computer Vision and Pattern Recognition, CVPR 2021, virtual, June 19-25, 2021*, pages 3558–3568. Computer Vision Foundation / IEEE, 2021. 9

[7] Junsong Chen, Jincheng Yu, Chongjian Ge, Lewei Yao, Enze Xie, Zhongdao Wang, James T. Kwok, Ping Luo, Huchuan Lu, and Zhenguo Li. Pixart- α : Fast training of diffusion transformer for photorealistic text-to-image synthesis. In *The Twelfth International Conference on Learning Representations, ICLR 2024, Vienna, Austria, May 7-11, 2024*. Open-Review.net, 2024. 3

[8] Juhai Chen, Zhiyang Xu, Xichen Pan, Yushi Hu, Can Qin, Tom Goldstein, Lifu Huang, Tianyi Zhou, Saining Xie, Silvio Savarese, Le Xue, Caiming Xiong, and Ran Xu. Blip3- α : A family of fully open unified multimodal models-architecture, training and dataset. *CoRR*, abs/2505.09568, 2025. 9

[9] Xi Chen, Xiao Wang, Lucas Beyer, Alexander Kolesnikov, Jialin Wu, Paul Voigtlaender, Basil Mustafa, Sebastian Goodman, Ibrahim Alabdulmohsin, Piotr Padlewski, Daniel Salz, Xi Xiong, Daniel Vlasic, Filip Pavetic, Keran Rong, Tianli Yu, Daniel Keysers, Xiaohua Zhai, and Radu Soricut. Pali-3 vision language models: Smaller, faster, stronger. *CoRR*, abs/2310.09199, 2023. 3

[10] Yanbei Chen, Shaogang Gong, and Loris Bazzani. Image search with text feedback by visiolinguistic attention learning. In *2020 IEEE/CVF Conference on Computer Vision and Pattern Recognition, CVPR 2020, Seattle, WA, USA, June 13-19, 2020*, pages 2998–3008. Computer Vision Foundation / IEEE, 2020. 1

[11] Ginger Delmas, Rafael Sampaio de Rezende, Gabriela Csurka, and Diane Larlus. ARTEMIS: attention-based retrieval with text-explicit matching and implicit similarity. In *The Tenth International Conference on Learning Representations, ICLR 2022, Virtual Event, April 25-29, 2022*. Open-Review.net, 2022. 1

[12] Rohit Girdhar, Alaaeldin El-Nouby, Zhuang Liu, Mannat Singh, Kalyan Vasudev Alwala, Armand Joulin, and Ishan Misra. Imagebind one embedding space to bind them all. In *IEEE/CVF Conference on Computer Vision and Pattern Recognition, CVPR 2023, Vancouver, BC, Canada, June 17-24, 2023*, pages 15180–15190. IEEE, 2023. 3

[13] Geonmo Gu, Sanghyuk Chun, Wonjae Kim, HeeJae Jun, Yoohoon Kang, and Sangdoo Yun. Compodiff: Versatile composed image retrieval with latent diffusion. *Trans. Mach. Learn. Res.*, 2024. 2, 3

[14] Geonmo Gu, Sanghyuk Chun, Wonjae Kim, Yoohoon Kang, and Sangdoo Yun. Language-only efficient training of zero-shot composed image retrieval. In *IEEE/CVF Conference on Computer Vision and Pattern Recognition, CVPR 2024, Seattle, WA, USA, June 16-22, 2024*, pages 13225–13234. IEEE, 2024. 5

[15] Jia-Wei Han, Sheng-Jie Luo, Zhe-Chen Xu, Ze-Yang Li, He-Ran Yang, and Dong-Ping Tian. Universal vision-language dense retrieval: Learning a unified representation space for multi-modal retrieval. *CoRR*, abs/2402.09415, 2024. 3

[16] Jonathan Ho, Ajay Jain, and Pieter Abbeel. Denoising diffusion probabilistic models. In *Advances in Neural Information Processing Systems 33: Annual Conference on Neural Information Processing Systems 2020, NeurIPS 2020, December 6-12, 2020, virtual*, pages 6840–6851, 2020. 3, 10, 11

[17] Mehrdad Hosseinzadeh and Yang Wang. Composed query image retrieval using locally bounded features. In *2020 IEEE/CVF Conference on Computer Vision and Pattern Recognition, CVPR 2020, Seattle, WA, USA, June 13-19, 2020*, pages 3593–3602. Computer Vision Foundation / IEEE, 2020. 1

[18] Mude Hui, Siwei Yang, Bingchen Zhao, Yichun Shi, Heng Wang, Peng Wang, Cihang Xie, and Yuyin Zhou. Hq-edit: A high-quality dataset for instruction-based image editing. In *The Thirteenth International Conference on Learning Representations, ICLR 2025, Singapore, April 24-28, 2025*. Open-Review.net, 2025. 9

[19] Chao Jia, Yinfei Yang, Ye Xia, Yi-Ting Chen, Zarana Parekh, Hieu Pham, Quoc V. Le, Yunhsuan Sung, Zhen Li, and Tom Duerig. Scaling up visual and vision-language representation learning with noisy text supervision. In *Proceedings of the 38th International Conference on Machine Learning*,

ICML 2021, 18-24 July 2021, Virtual Event, pages 4904–4916. PMLR, 2021. 3

[20] Shyamgopal Karthik, Karsten Roth, Massimiliano Mancini, and Zeynep Akata. Vision-by-language for training-free compositional image retrieval. In *The Twelfth International Conference on Learning Representations, ICLR 2024, Vienna, Austria, May 7-11, 2024*. OpenReview.net, 2024. 2, 3, 5, 11, 13, 15

[21] Jongseok Kim, Youngjae Yu, Hoeseong Kim, and Gunhee Kim. Dual compositional learning in interactive image retrieval. In *Thirty-Fifth AAAI Conference on Artificial Intelligence, AAAI 2021, Thirty-Third Conference on Innovative Applications of Artificial Intelligence, IAAI 2021, The Eleventh Symposium on Educational Advances in Artificial Intelligence, EAAI 2021, Virtual Event, February 2-9, 2021*, pages 1771–1779. AAAI Press, 2021. 1

[22] Diederik P. Kingma and Jimmy Ba. Adam: A method for stochastic optimization. In *3rd International Conference on Learning Representations, ICLR 2015, San Diego, CA, USA, May 7-9, 2015, Conference Track Proceedings*, 2015. 11

[23] Alexander Kirillov, Eric Mintun, Nikhila Ravi, Hanzi Mao, Chloé Rolland, Laura Gustafson, Tete Xiao, Spencer Whitehead, Alexander C. Berg, Wan-Yen Lo, Piotr Dollár, and Ross B. Girshick. Segment anything. In *IEEE/CVF International Conference on Computer Vision, ICCV 2023, Paris, France, October 1-6, 2023*, pages 3992–4003. IEEE, 2023. 9

[24] Seungmin Lee, Dongwan Kim, and Bohyung Han. Cosmo: Content-style modulation for image retrieval with text feedback. In *IEEE Conference on Computer Vision and Pattern Recognition, CVPR 2021, virtual, June 19-25, 2021*, pages 802–812. Computer Vision Foundation / IEEE, 2021. 1

[25] Junnan Li, Dongxu Li, Silvio Savarese, and Steven C. H. Hoi. BLIP-2: bootstrapping language-image pre-training with frozen image encoders and large language models. In *International Conference on Machine Learning, ICML 2023, 23-29 July 2023, Honolulu, Hawaii, USA*, pages 19730–19742. PMLR, 2023. 3

[26] You Li, Fan Ma, and Yi Yang. Imagine and seek: Improving composed image retrieval with an imagined proxy. In *IEEE/CVF Conference on Computer Vision and Pattern Recognition, CVPR 2025, Nashville, TN, USA, June 11-15, 2025*, pages 3984–3993. Computer Vision Foundation / IEEE, 2025. 2, 3, 5

[27] Zehan Li, Xin Zhang, Yanzhao Zhang, Dingkun Long, Pengjun Xie, and Meishan Zhang. Towards general text embeddings with multi-stage contrastive learning. *CoRR*, abs/2308.03281, 2023. 3

[28] Zheyuan Liu, Cristian Rodriguez Opazo, Damien Teney, and Stephen Gould. Image retrieval on real-life images with pre-trained vision-and-language models. In *2021 IEEE/CVF International Conference on Computer Vision, ICCV 2021, Montreal, QC, Canada, October 10-17, 2021*, pages 2105–2114. IEEE, 2021. 1, 5, 9

[29] Cheng Lu, Yuhao Zhou, Fan Bao, Jianfei Chen, Chongxuan Li, and Jun Zhu. Dpm-solver++: Fast solver for guided sampling of diffusion probabilistic models. *Mach. Intell. Res.*, 22(4):730–751, 2025. 11

[30] Sheng-Jie Luo, Jia-Wei Han, Tao-Rui-Chi Yu, Ze-Yang Li, and He-Ran Yang. Mm-embed: A unified embedding space for multi-modal retrieval and generative large models. *CoRR*, abs/2403.09551, 2024. 3

[31] Chenlin Meng, Yutong He, Yang Song, Jiaming Song, Jiajun Wu, and Stefano Ermon. Sdedit: Guided image synthesis and editing with stochastic differential equations. In *10th International Conference on Learning Representations, ICLR 2022, Virtual Event, April 25-29, 2022*. OpenReview.net, 2022. 3

[32] William Peebles and Saining Xie. Scalable diffusion models with transformers. In *IEEE/CVF International Conference on Computer Vision, ICCV 2023, Paris, France, October 1-6, 2023*, pages 4172–4182. IEEE, 2023. 9

[33] Alec Radford, Jong Wook Kim, Chris Hallacy, Aditya Ramesh, Gabriel Goh, Sandhini Agarwal, Girish Sastry, Amanda Askell, Pamela Mishkin, Jack Clark, Gretchen Krueger, and Ilya Sutskever. Learning transferable visual models from natural language supervision. In *Proceedings of the 38th International Conference on Machine Learning, ICML 2021, 18-24 July 2021, Virtual Event*, pages 8748–8763. PMLR, 2021. 3

[34] Robin Rombach, Andreas Blattmann, Dominik Lorenz, Patrick Esser, and Björn Ommer. High-resolution image synthesis with latent diffusion models. In *IEEE/CVF Conference on Computer Vision and Pattern Recognition, CVPR 2022, New Orleans, LA, USA, June 18-24, 2022*, pages 10674–10685. IEEE, 2022. 3

[35] Chitwan Saharia, William Chan, Saurabh Saxena, Lala Li, Jay Whang, Emily L. Denton, Seyed Kamyar Seyed Ghasemipour, Raphael Gontijo Lopes, Burcu Karagol Ayan, Tim Salimans, Jonathan Ho, David J. Fleet, and Mohammad Norouzi. Photorealistic text-to-image diffusion models with deep language understanding. In *Advances in Neural Information Processing Systems 35: Annual Conference on Neural Information Processing Systems 2022, NeurIPS 2022, New Orleans, LA, USA, November 28 - December 9, 2022*, 2022. 3

[36] Kuniaki Saito, Kihyuk Sohn, Xiang Zhang, Chun-Liang Li, Chen-Yu Lee, Kate Saenko, and Tomas Pfister. Pic2word: Mapping pictures to words for zero-shot composed image retrieval. In *IEEE/CVF Conference on Computer Vision and Pattern Recognition, CVPR 2023, Vancouver, BC, Canada, June 17-24, 2023*, pages 19305–19314. IEEE, 2023. 1, 2, 5

[37] Jiaming Song, Chenlin Meng, and Stefano Ermon. Denoising diffusion implicit models. In *9th International Conference on Learning Representations, ICLR 2021, Virtual Event, Austria, May 3-7, 2021*. OpenReview.net, 2021. 3

[38] Keqiang Sun, Junting Pan, Yuying Ge, Hao Li, Haodong Duan, Xiaoshi Wu, Renrui Zhang, Aojun Zhou, Zipeng Qin, Yi Wang, Jifeng Dai, Yu Qiao, Limin Wang, and Hongsheng Li. Journeydb: A benchmark for generative image understanding. In *Advances in Neural Information Processing Systems 36: Annual Conference on Neural Information Processing Systems 2023, NeurIPS 2023, New Orleans, LA, USA, December 10 - 16, 2023*, 2023. 9

[39] Yuanmin Tang, Jing Yu, Keke Gai, Jiamin Zhuang, Gang Xiong, Yue Hu, and Qi Wu. Context-i2w: Mapping images

to context-dependent words for accurate zero-shot composed image retrieval. In *Thirty-Eighth AAAI Conference on Artificial Intelligence, AAAI 2024, Thirty-Sixth Conference on Innovative Applications of Artificial Intelligence, IAAI 2024, Fourteenth Symposium on Educational Advances in Artificial Intelligence, EAAI 2014, February 20-27, 2024, Vancouver, Canada*, pages 5180–5188. AAAI Press, 2024. 1

[40] Yuanmin Tang, Jue Zhang, Xiaoting Qin, Jing Yu, Gaopeng Gou, Gang Xiong, Qingwei Lin, Saravan Rajmohan, Dongmei Zhang, and Qi Wu. Reason-before-retrieve: One-stage reflective chain-of-thoughts for training-free zero-shot composed image retrieval. In *IEEE/CVF Conference on Computer Vision and Pattern Recognition, CVPR 2025, Nashville, TN, USA, June 11-15, 2025*, pages 14400–14410. Computer Vision Foundation / IEEE, 2025. 2, 3, 5

[41] Nam Vo, Lu Jiang, Chen Sun, Kevin Murphy, Li-Jia Li, Li Fei-Fei, and James Hays. Composing text and image for image retrieval - an empirical odyssey. In *IEEE Conference on Computer Vision and Pattern Recognition, CVPR 2019, Long Beach, CA, USA, June 16-20, 2019*, pages 6439–6448. Computer Vision Foundation / IEEE, 2019. 1

[42] Liang Wang, Nan Yang, Xiaolong Huang, Linjun Yang, Ranjan Majumder, and Furu Wei. Improving text embeddings with large language models. In *Proceedings of the 62nd Annual Meeting of the Association for Computational Linguistics (Volume 1: Long Papers), ACL 2024, Bangkok, Thailand, August 11-16, 2024*, pages 11897–11916. Association for Computational Linguistics, 2024. 3

[43] Lan Wang, Wei Ao, Vishnu Naresh Boddeti, and Ser-Nam Lim. Generative zero-shot composed image retrieval. In *IEEE/CVF Conference on Computer Vision and Pattern Recognition, CVPR 2025, Nashville, TN, USA, June 11-15, 2025*, pages 29690–29700. Computer Vision Foundation / IEEE, 2025. 2, 3, 5, 11, 13, 15

[44] Hui Wu, Yupeng Gao, Xiaoxiao Guo, Ziad Al-Halah, Steven Rennie, Kristen Grauman, and Rogério Feris. Fashion IQ: A new dataset towards retrieving images by natural language feedback. In *IEEE Conference on Computer Vision and Pattern Recognition, CVPR 2021, virtual, June 19-25, 2021*, pages 11307–11317. Computer Vision Foundation / IEEE, 2021. 5, 9

[45] Enze Xie, Junsong Chen, Yuyang Zhao, Jincheng Yu, Ligeng Zhu, Yujun Lin, Zhekai Zhang, Muyang Li, Junyu Chen, Han Cai, Bingchen Liu, Daquan Zhou, and Song Han. SANA 1.5: Efficient scaling of training-time and inference-time compute in linear diffusion transformer. *CoRR*, abs/2501.18427, 2025. 3, 6

[46] Zhenyu Yang, Dizhan Xue, Shengsheng Qian, Weiming Dong, and Changsheng Xu. LDRE: llm-based divergent reasoning and ensemble for zero-shot composed image retrieval. In *Proceedings of the 47th International ACM SIGIR Conference on Research and Development in Information Retrieval, SIGIR 2024, Washington DC, USA, July 14-18, 2024*, pages 80–90. ACM, 2024. 5

[47] Lvmin Zhang, Anyi Rao, and Maneesh Agrawala. Adding conditional control to text-to-image diffusion models. In *IEEE/CVF International Conference on Computer Vision, ICCV 2023, Paris, France, October 1-6, 2023*, pages 3813–3824. IEEE, 2023. 3

[48] Xin Zhang, Yanzhao Zhang, Wen Xie, Mingxin Li, Ziqi Dai, Dingkun Long, Pengjun Xie, Meishan Zhang, Wenjie Li, and Min Zhang. Bridging modalities: Improving universal multimodal retrieval by multimodal large language models. In *IEEE/CVF Conference on Computer Vision and Pattern Recognition, CVPR 2025, Nashville, TN, USA, June 11-15, 2025*, pages 9274–9285. Computer Vision Foundation / IEEE, 2025. 3